Optics Letters

Time-resolved multimode heterodyne detection for dissecting coherent states of matter

Filippo Glerean,[1,2] Giacomo Jarc,[1,2] Alexandre Marciniak,[1,2] Francesca Giusti,[1,2] Giorgia Sparapassi,[1,2] Angela Montanaro,[1,2] Enrico Maria Rigoni,[1,2] Jonathan Owen Tollerud,[1,2,3] and Daniele Fausti[1,2,4,*]

[1]*Dipartimento di Fisica, Università degli Studi di Trieste, Via Valerio 2, Trieste I-34127, Italy*
[2]*Sincrotrone Trieste S.C.p.A., Basovizza I-34127, Italy*
[3]*Optical Sciences Centre, Swinburne University, 1 Alfred Street, Hawthorn, VIC 3122, Australia*
[4]*Department of Chemistry, Princeton University, Princeton, New Jersey 08544, USA*
Corresponding author: daniele.fausti@elettra.eu

Unveiling and controlling the time evolution of the momentum and position of low energy excitations such as phonons, magnons, and electronic excitation is the key to attain coherently driven new functionalities of materials. Here we report the implementation of femtosecond time- and frequency-resolved multimode heterodyne detection and show that it allows for independent measurement of the time evolution of the position and momentum of the atoms in coherent vibrational states in α-quartz. The time dependence of the probe field quadratures reveals that their amplitude is maximally changed when the atoms have maximum momentum, while their phase encodes a different information and evolves proportionally to the instantaneous atomic positon. We stress that this methodology, providing the mean to map both momentum and position in one optical observable, may be of relevance for both quantum information technologies and time-domain studies on complex materials. © 2020 Optical Society of America

The Raman response of materials and molecules is commonly measured in time domain through pump and probe (P&P) experiments relying on impulsive stimulated Raman scattering (ISRS). The most commonly employed scheme, dubbed one-dimensional P&P, uses two ultrashort light pulses: the first pulse (pump) excites the system, while the second (probe), impinging on the sample at a controllable time delay, measures the time evolution of the non-equilibrium state. The measurement of the Raman response in P&P experiments relies on the fact that impulsive photo-excitation (i.e., the interaction with light pulses on a timescale shorter than the period of the excitation in the material) triggers coherent non-equilibrium states of low energy excitations, such as phonons [1,2], magnons [3], or electronic excitations [4–6], whose time evolution can be subsequently characterized by the ultrashort probe pulse. It should be noted that the majority of the experiments studying spectrally resolved P&P response must tolerate a high intensity probe, comprising sufficiently high intensity in each spectral component [7,8].

ISRS has been historically introduced and discussed treating only the high intensity limit where both the coherent vibrational state in matter, which is often dubbed coherent phonon, and the interacting electric field are described in a classical formalism [9–11]. However, more recently, ISRS processes have emerged as a powerful tool for quantum information, and it has been shown that ISRS can be at play even with relatively weak pulses and be used to store/retrieve single photons in/from the elastic field of materials [12,13] as well as frequency convert single photons through nonlinear processes that can occur in probe pulses containing only a few photons [14,15]. In this context, a growing interest in studying coherent non-equilibrium Raman dynamics with low intensity pulses is emerging.

Optical heterodyne detection (OHD) is a linear interferential method commonly used in equilibrium and time domain optical measurements to reveal weak light beams. In OHD, a weak signal is amplified by the interference with a strong local oscillator (LO). The phase-locked LO acts as an amplifier and enables the direct measurement of the amplitude and phase of the signal with improved sensitivity and high signal-to-noise ratio [16–25].

In this Letter, we report the first study of non-equilibrium coherent vibrational response in α-quartz by means of P&P studies combined with pulse shaping and spectrally selective optical heterodyne measurements of the few photon probe light pulses. The setup developed (sketched in Fig. 1) combines femtosecond spectroscopy, interferometric balanced heterodyne detection, and pulse shaping, which allow us to measure the time evolution of the quadrature (amplitude and phase) of each weak probe spectral component (100s photons) driven by a coherent vibrational response. We stress that with the proposed methodology, the time and frequency resolution are determined independently respectively by the P&P duration at the sample and the frequency resolution of the pulse shaper. Disentangling the time and wavelength dependence of the spectral phase and amplitude, with a time resolution higher than the vibrational
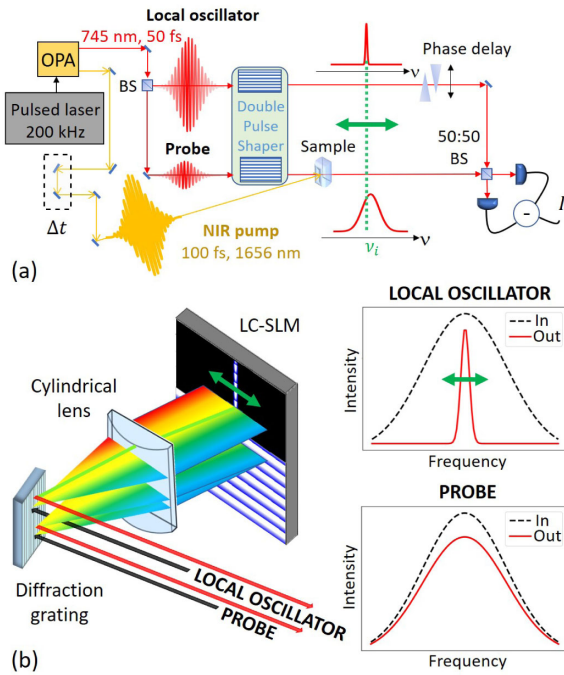
Fig. 1. Experimental details. (a) Layout of the optical setup employed for time-resolved multimode heterodyne detection. It consists of a pump–probe experiment where the signal field out of the sample is amplified and referenced with a local oscillator shaped in its spectral content. (b) Two-beam diffraction-based pulse shaper using a 2D phase-only spatial light modulator.

cycle, allows us to distinguish between two qualitatively different effects of the coherent phonon response in α-quartz. This provides unique insight into the coherent evolution of the atomic position, which is not attainable in standard P&P measurements. In detail, the amplitude measurements reveal that the intra-pulse spectral density is dynamically redistributed due to light–phonon energy exchanges, which are mediated by the time evolution of the momentum of the atoms. On the contrary, the phase is sensitive to a linear modulation of the refractive properties of the material, which are proportional to the atom displacement. This could be indicative of changes in the inductive response due to the renormalization of high energy oscillators associated with the electronic gap. Importantly, the dynamics of the spectral phase yields a robust observable even in measurements with probe pulses with few photons. This indicates that the method proposed can both provide new physical insight into the coherent evolution of the vibrational states and improve the detection of coherent responses with respect to standard intensity-based measurements. By providing access to these unique features, this time-resolved multimode heterodyne detection scheme may be advantageous for a broad class of non-equilibrium experiments, from condensed matter to molecular physics.

The experiment combines ultrafast pump–probe spectroscopy and multimode heterodyne detection of the probe field. The layout of the optical setup is shown in Fig. 1(a) (polarization control and focusing elements are not shown). P&P pulses are produced by a commercial 200 kHz pulsed laser + optical parametric amplifier (OPA) system (Pharos + Orpheus-F, Light Conversion). The signal from the OPA used as the probe and

heterodyning field in the interferometer has a duration <50 fs and a tunable wavelength in the range of 650–950 nm. The idler is used as the pump and has a duration <100 fs and wavelength in the near-infrared range. The experiments reported are performed with a probe (pump) wavelength of 745 nm (1656 nm). P&P both lie in the sample transparency range and have the same polarization. The weak probe signal field interferes in a Mach–Zehnder scheme together with a more intense and phase-locked LO field, which acts as the amplifier and phase reference. The outputs of the 50:50 beam splitter are acquired pulse by pulse with a differential detector subtracting the response from two photodiodes. The difference between the two photo-voltages (heterodyne trace) is measured with a low noise charge amplifier and then digitized. It can be shown that the mean value of the differential current $\langle I \rangle$ as a function of the LO phase maps the mean phase-resolved quadrature of the probe field $\langle X \rangle$, which is the representative observable of the complex electric field.

Indeed, by denoting with z_ν the amplitude of the single-mode LO of frequency ν, with ϕ_ν^{LO} its tunable phase and with $\alpha_\nu = |\alpha_\nu| e^{i\phi_\nu}$ the complex amplitude of each probe mode, the heterodyne current reads

$$\langle I \rangle = \sqrt{2} d\nu' |z_{\nu'}| \langle X_{\nu'}(\phi_{\nu'} - \phi_{\nu'}^{LO}) \rangle$$

$$= \int d\nu' |z_{\nu'}| (\alpha_{\nu'} e^{-i\phi_{\nu'}^{LO}} + \alpha_{\nu'}^* e^{+i\phi_{\nu'}^{LO}})$$

$$= 2 \int d\nu' |\alpha_{\nu'}||z_{\nu'}| \cos(\phi_{\nu'} - \phi_{\nu'}^{LO}). \tag{1}$$

In order to achieve frequency resolution, we select a narrow spectral band in the LO (approximated by a delta function, $z_{\nu'} = z_\nu \delta_{\nu,\nu'}$), which defines the heterodyne amplification of probe frequency ν. Thus, the measured observable for each frequency mode is

$$\langle I \rangle_\nu = 2 |\alpha_\nu||z_\nu| \cos(\phi_\nu - \phi_\nu^{LO}). \tag{2}$$

The data recorded as a function of the relative phase between LO and signal consist of a sinusoidal oscillation at frequency ν [Fig. 2(a)]. The oscillation amplitude is proportional to the signal field amplitude, scaled by the LO field.

In the experiment, the LO narrow spectral band is selected by a diffraction based pulse shaper [26–28] [Fig. 1(b)], which allows for independent control of the amplitude and phase of each spectral component of the LO and the probe. The horizontally dispersed spectral components are focused on a two-dimensional liquid crystal-spatial light modulator (LC-SLM) (Santec SLM-100) that consists of a multipixel array of nematic crystals used to generate programmable blazed diffraction gratings. The programmable vertical position and the depth of the grating for all spectral components are used to control, respectively, the spectral phase and the amplitude of the diffracted beam. In particular, as depicted in Fig. 1(b), applying a blazed pattern only to specific horizontal positions results in a narrowband diffracted LO.

In the experiment reported here, the pulse shaper is used to narrow the LO to the width of a single mode, with a tunable central frequency and resolution of 0.1 THz. As illustrated in Fig. 1(b), the probe is also shaped. The choice of common optics between LO and probe improves the interferometer stability,
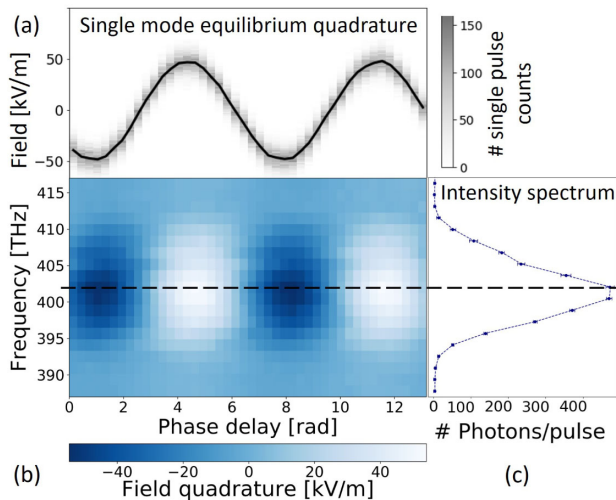
Fig. 2. Equilibrium heterodyne spectral trace. (a) Single-mode quadrature in units of electric field at the sample focus; distribution of single pulse counts (gray histograms) and mean value (solid line). (b) Spectral quadrature map. (c) Corresponding intensity spectrum: we employ probe pulses with a few hundred photons per selected mode.

Fig. 3. Time-resolved vibrational dynamics. (a) Sketch of non-equilibrium amplitude (a1) and phase (a2) quadrature modulations. (b) Spectral maps of coherent phonon oscillations in quartz for amplitude (b1) and phase (b2). (c) The amplitude response has opposite behavior on the two sides of the spectrum, while the phase response is the same across the spectrum and is shifted by $\pi/2$ (see dashed vertical guide). The error bars (1σ) indicate that the phase detection grants a better signal-to-noise ratio with respect to amplitude measurements. Fourier transform analysis of the time traces (insert) shows the detected phonons' frequencies.

and the capability of the LC-SLM to modulate the phase of each spectral component can be exploited to correct the probe temporal compression and its chirp. The reconstruction of the quadrature on the entire spectral range is performed by scanning the LO across the different frequency components. For each selected mode, we measure the heterodyne oscillation trace [Eq. (2), Fig. 2(a)], and by scanning the LO frequencies, we obtain the spectral map in Fig. 2(b). For each component, we proceed to fit its amplitude and phase. Taking into account that the employed LO has the same spectral shape as the probe, i.e., $z_\nu \propto \alpha_\nu$, we can renormalize the heterodyne oscillation amplitude and get the probe amplitude spectrum. By squaring it, we can obtain the intensity of each spectral component ($I = |\alpha|^2$) in Fig. 2(c). In order to perform a quantitative estimation, we record the intensity of the signal and LO beams with a power meter. We employ a 402 THz (745 nm) beam and 20 THz bandwidth. The probe has 5 fJ per pulse (10^4 photons). The LO is three orders of magnitude more intense: 5 pJ, 10^7 photons. The single modes are obtained with a 0.25 THz bandwidth filter, and for the central LO mode, we have 0.12 pJ, 10^6 photons. All this considered, acquiring 2000 pulse repetitions for each LO phase point and sampling the quadrature oscillation with 0.25 rad steps, we can reconstruct the mean value intensity spectrum with a few hundreds of photons per mode. We estimate an uncertainty of ± 3 photons at the spectrum peak and ± 1 on the tails by calculating the standard deviation on the results of 10 independent acquisitions.

We apply multimode heterodyne detection in the time domain to address the coherent evolution of lattice vibrations in non-absorbing media by studying how the probe–phonon interaction is mapped into the spectral modifications (amplitude and phase) of each probe frequency component [Fig. 3(a)]. Transparent media (as α-quartz) represent benchmark systems for this study, since no electronic transitions are dipole allowed within the pump or probe bandwidth, and the probe–matter interaction can be treated as an effective photon–phonon coupling [9–11,15–17].
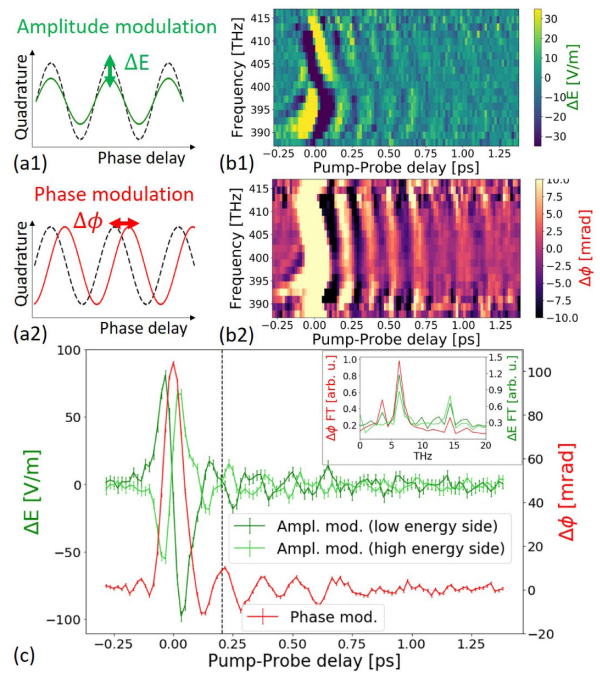
The energy transfer in photon–phonon interaction is mediated by non-resonant ISRS [9,15–17], which is an intrinsic multimode process occurring whenever an ultrashort pulse (with a bandwidth greater than the excited phonon frequency Ω) propagates in a Raman-active medium. All optical modes in the optical pulse with an energy difference corresponding to $\hbar\Omega$ can interact and create (Stokes Raman process) or annihilate (anti-Stokes) a phonon.

The coherent vibrational states are excited via ISRS by the intense pump pulse (fluence 10 mJ/cm²). The time-dependent modulations of the spectral amplitude and phase of the weak probe (50 pJ/cm²) are presented in Fig. 3(b). The latter are obtained by separately fitting the pumped and equilibrium heterodyne current with a sinusoidal function for combination of delay and frequency, and then we evaluate the differential amplitude and phase from the fitted parameters. We use a chopper blade on the pump beam to simultaneously reference the fluctuations in the equilibrium response, and in this way, we can observe spectral variations with a sensitivity of two photons per pulse, and a phase stability of 2 mrad (standard deviation).

We observe an oscillation in time of the response of both amplitude and phase at the frequency of the excited phonon modes. Interestingly, the amplitude and phase responses are out of phase and reveal two different responses, representative of two typologies of interaction, ruled by the coherent phonon phase [15]. In particular, as highlighted in Fig. 3(c), the amplitude is modulated with opposite signs on the two sides of the probe

spectral bandwidth. This is a general feature of ISRS [2,9,15] and indicates a dynamical spectral weight redistribution within the probe bandwidth. If the probe interacts with the coherent vibrational state at a time when the atoms have the maximum momentum, the Stokes process dominates and high frequency photons are down-converted. On the contrary, when the probe impinges on the sample when the atoms are coherently moving with minimum momentum, a partial quench of the atomic motion can be triggered and the probe–phonon interaction is dominated by the anti-Stokes process, i.e., low frequency photons are up-converted, and an effective energy transfer between the elastic field and the probe occurs. Conversely, the time dependence of the phase of the spectral components exhibits a uniform behavior across the probe spectrum, and it is $\pi/2$ shifted with respect to the amplitude oscillation. This indicates that the phase response results from the linear modulation of the sample refractive properties. The real part of the refractive index is dependent on the lattice displacements, and the time domain response of the phase is ruled by the coherently evolving atom position. This is consistent with a change in a high energy optical property (such as the gap) that is proportional to the instantaneous atomic position and that would result in a uniform change in the inductive response at frequencies smaller than the optical gap. This intriguing scenario should be confirmed in future studies of the time-dependent high energy absorption.

Quantitatively, the experiment is performed with a few hundreds of photons in the probe bandwidth selected by the LO, and the intensity modulations range from one to 10 photons. We highlight that the time-domain response of the phase gives a significantly better signal-to-noise ratio than the amplitude. This can be understood by considering that the pump-induced amplitude modulation is due to a small fraction of scattered photons, while the phase modulation is the result of a process that involves the entire probe beam. This suggests that in the low probe photon number, phase modulation is a more suitable observable compared with amplitude or intensity dynamics.

In this Letter, we present time-resolved multimode heterodyne detection and measure non-equilibrium dynamics associated with a coherent vibrational response in a prototypical sample (α-quartz) in the probe low photon number regime.

As a perspective, the fact that quantitatively we work with a few hundreds of photons per frequency mode means we can access the shot noise regime, where the probe photon statistics is dominated by quantum fluctuations, which overcome the classical instabilities (which scale linearly on the order of 0.1–1% for our laser source). Reaching the shot noise limited regime enables to perform full quantum state reconstruction of the optical field and to merge the analysis of statistical degrees of freedom of light with ultrafast non-equilibrium processes [29]. In particular, ISRS is an intrinsically multimode process that imparts correlation among the different spectral components coupled through the phonon modes [30] and could represent a new platform to build and manipulate multimode entanglement within the bandwidth in optical pulses [31].

Disclosures. The authors declare no conflicts of interest.

REFERENCES

1. M. Hase, K. Mizoguchi, H. Harima, S. Nakashima, M. Tani, K. Sakai, and M. Hangyo, Appl. Phys. Lett. **69**, 2474 (1996).
2. K. G. Nakamura, K. Ohya, H. Takahashi, T. Tsuruta, H. Sasaki, S.-I. Uozumi, K. Norimatsu, M. Kitajima, Y. Shikano, and Y. Kayanuma, Phys. Rev. B **94**, 024303 (2016).
3. T. Kampfrath, A. Sell, G. Klatt, A. Pashkin, S. Mährlein, T. Dekorsy, M. Wolf, M. Fiebig, A. Leitenstorfer, and R. Huber, Nat. Photonics **5**, 31 (2010).
4. D. M. Sagar, A. A. Tsvetkov, D. Fausti, S. van Smaalen, and P. H. M. van Loosdrecht, J. Phys. Condens. Matter **19**, 346208 (2007).
5. D. Werdehausen, T. Takayama, M. Höppner, G. Albrecht, A. W. Rost, Y. Lu, D. Manske, H. Takagi, and S. Kaiser, Sci. Adv. **4**, eaap8652 (2018).
6. B. Mansart, J. Lorenzana, A. Mann, A. Odeh, M. Scarongella, M. Chergui, and F. Carbone, Proc. Natl. Acad. Sci. USA **110**, 4539 (2013).
7. F. Randi, I. Vergara, F. Novelli, M. Esposito, M. Dell'Angela, V. A. M. Brabers, P. Metcalf, R. Kukreja, H. A. Dürr, D. Fausti, M. Grüninger, and F. Parmigiani, Phys. Rev. B **93**, 054305 (2016).
8. F. Novelli, G. D. Filippis, V. Cataudella, M. Esposito, I. Vergara, F. Cilento, E. Sindici, A. Amaricci, C. Giannetti, D. Prabhakaran, S. Wall, A. Perucchi, S. D. Conte, G. Cerullo, M. Capone, A. Mishchenko, M. Grüninger, N. Nagaosa, F. Parmigiani, and D. Fausti, Nat. Commun. **5**, 5112 (2014).
9. Y.-X. Yan, E. B. Gamble, and K. A. Nelson, J. Chem. Phys. **83**, 5391 (1985).
10. R. Merlin, Solid State Commun. **102**, 207 (1997).
11. T. E. Stevens, J. Kuhl, and R. Merlin, Phys. Rev. B **65**, 144304 (2002).
12. K. C. Lee, M. R. Sprague, B. J. Sussman, J. Nunn, N. K. Langford, X.-M. Jin, T. Champion, P. Michelberger, K. F. Reim, D. England, D. Jaksch, and I. A. Walmsley, Science **334**, 1253 (2011).
13. D. G. England, K. A. Fisher, J.-P. W. MacLean, P. J. Bustard, R. Lausten, K. J. Resch, and B. J. Sussman, Phys. Rev. Lett. **114**, 053602 (2015).
14. K. A. G. Fisher, D. G. England, J.-P. W. MacLean, P. J. Bustard, K. J. Resch, and B. J. Sussman, Nat. Commun. **7**, 11200 (2016).
15. F. Glerean, S. Marcantoni, G. Sparapassi, A. Blason, M. Esposito, F. Benatti, and D. Fausti, J. Phys. B **52**, 145502 (2019).
16. F. Benatti, M. Esposito, D. Fausti, R. Floreanini, K. Titimbo, and K. Zimmermann, New J. Phys. **19**, 023032 (2017).
17. M. Esposito, K. Titimbo, K. Zimmermann, F. Giusti, F. Randi, D. Boschetto, F. Parmigiani, R. Floreanini, F. Benatti, and D. Fausti, Nat. Commun. **6**, 10249 (2015).
18. D. N. Fittinghoff, J. L. Bowie, J. N. Sweetser, R. T. Jennings, M. A. Krumbügel, K. W. DeLong, R. Trebino, and I. A. Walmsley, Opt. Lett. **21**, 884 (1996).
19. T. Fuji, T. Yoda, T. Hattori, and H. Nakatsuka, Jpn. J. Appl. Phys. **39**, 1738 (2000).
20. E. Tokunaga, A. Terasaki, and T. Kobayashi, J. Opt. Soc. Am. B **12**, 753 (1995).
21. L. Lepetit, G. Chériaux, and M. Joffre, J. Opt. Soc. Am. B **12**, 2467 (1995).
22. M. Cooper, C. Söller, and B. J. Smith, J. Mod. Opt. **60**, 611 (2013).
23. H. R. Carleton and W. T. Maloney, Appl. Opt. **7**, 1241 (1968).
24. G. L. Abbas, V. W. S. Chan, and T. K. Yee, Opt. Lett. **8**, 419 (1983).
25. C. Dorrer, P. Londero, and I. A. Walmsley, Opt. Lett. **26**, 1510 (2001).
26. A. M. Weiner, Rev. Sci. Instruments **71**, 1929 (2000).
27. J. C. Vaughan, T. Hornung, T. Feurer, and K. A. Nelson, Opt. Lett. **30**, 323 (2005).
28. A. Monmayrant, S. Weber, and B. Chatel, J. Phys. B **43**, 103001 (2010).
29. N. B. Grosse, N. Owschimikow, R. Aust, B. Lingnau, A. Koltchanov, M. Kolarczik, K. Lüdge, and U. Woggon, Opt. Express **22**, 32520 (2014).
30. J. O. Tollerud, G. Sparapassi, A. Montanaro, S. Asban, F. Glerean, F. Giusti, A. Marciniak, G. Kourousias, F. Billè, F. Cilento, S. Mukamel, and D. Fausti, Proc. Natl. Acad. Sci. USA **116**, 5383 (2019).
31. J. Roslund, R. M. de Araújo, S. Jiang, C. Fabre, and N. Treps, Nat. Photonics **8**, 109 (2013).